Nuclear Science & Technology Research Institute

Journal of Nuclear Research and Applications

Technical Paper

Journal homepage: http://jonra.nstri.ir

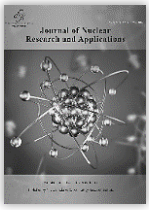

Evalution of Minimum Detection Activity in a Portable whole Body Counter Using Monte Carlo Method

H. Poorbaygi[1]*, S. Pourali[2], K. Moradi[1]

[1] Radiation Application Research School, Nuclear Science and Technology Research Institute, P. O. Box: 11365-3486, Tehran, Iran.
[2] Faculty of Advanced Science & Technologies, University of Isfahan, P. O. Box: 8174673441, Isfahan, Iran.

(Received: 29 August 2023, Revised: 9 January 2024, Accepted: 22 January 2024)

ABSTRACT

A portable body counter detects internal contamination in an emergency. Monte Carlo code estimates minimum detection activity (MDA) for a portable whole-body counter. In the case of outdoor open fields, natural background radiations were simulated. This counter has a chair geometry equipped with a NaI (Tl) detector (5cm x 5cm) inside a lead shield collimator consisting of a set of lines and a continuous component with monenergistic γ sources ranging from 300 to 2000 keV at intervals of 100 keV. This data matrix is folded with the measured spectrum outside the setup to estimate the observed spectrum in the detector. We evaluated the variation of the detector flux transmitted through the lead collimator and chair shield. This was done at different lead densities and different photon energies. Computational data were used to estimate the monitoring system MDA. This method is cheaper to design and test a counter system for low-level counting of γ emitting radionuclides than experimental methods.

Keywords: Body counter, Monte carlo simulations, Phantom, Efficiency, Minimum detectable activity.

1. Introductions

Whole-body counters are used for direct measurements of internal contamination and to evaluate internal dosimetry [1-3]. They often include NaI (Tl) detectors, which are high-efficiency and cost-effective [2, 4]. The BOMAB phantom is widely used for energy calibration and body counter efficiency [5]. The efficiency of the detector depends on the density and size of the detector material, the type and energy of the radiation, and the electronics [6–12]. The minimum detectable level of radioactivity (MDA) is very critical in gamma spectrometry setup and is related to the accuracy of internal contamination measurements using whole-body counters [13]. This parameter is qualitatively inversely related to background radiation level and has a direct relationship with detector efficiency. Background radiation

* Corresponding Author E-mail: hpoorbaygi@gmail.com
DOI: https://doi.org/10.24200/jon.2024.1004.

effects are significant enough in typical detector applications, as most detectors provide a certain amount of shielding for the detector to reduce background effects and separate it from the laboratory environment [14, 15]. Designing and testing new equipment is expensive and time-consuming. In these cases, the Monte Carlo simulation results are useful as a model for design purposes [16–19]. Analyzing the effects of different physical parameters on the activity by simulation [16]. These calculations are performed to determine the optimum size of the detector and the effect of counting geometry on body monitoring for radionuclides. For example, Kramer et al. presented a Monte Carlo simulation study for a whole-body counting system with the geometry of a chair equipped with a NaI (Tl) detector (29.2 cm in diameter, 10.2 cm in height) in a shielded room. The geometry of the detection in this simulation is such that the Bottle Mannequin Absorber (BOMAB) phantom is placed on a chair at an angle of 45 o and a distance of 71 cm, and the source has a uniform distribution in the phantom using Monte Carlo simulation [20]. Lei et al. developed a portable internal contamination monitor with a dual detector (3-inch NaI (Tl) detector) that was developed with considerable MDA and low cost and is suitable for large-scale applications [21].

A monitoring system with chair-type geometry has been designed and manufactured using a Nal (Tl) detector (5cm in diameter ×5cm in height) with a lead collimator, and the chair is shielded using a 5cm thick lead layer [22]. In the previous article, a whole-body counter with chair geometry including a detector and a local shield was made and its calibration was done with a phantom. But in this study, we want a computational study to estimate the MDA of this type of counter. This also depends on the type of source of background radiation.

The study investigates the use of the Monte Carlo method to define a source for actual background radiation. In the next step, as an application, we evaluate the counting efficiency of a chair-type body counter with a BOMAB phantom.

2. Theories and computational method

2.1 Design method

MDA is a good measure of detector performance [16], and it depends on both counting efficiency and background radiation, as shown in the following expression:

$$\mathrm{MDA} = \frac{4.653\sqrt{\mathrm{Bg}}}{\mathrm{T}\times\mathrm{E}} \quad (1)$$

Where Bg is the background counts in the region of interest, f is the abundance percentage, E is counting efficiency (cps Bq^{-1}), and T is counting time (sec) [16].

The detector response is calculated using mono-energetic gamma sources as isotropic spherical surface sources that surround the detector and seat shield. This is done to simulate the geometry of the incoming background radiation from the environment toward the detector. The source input is comprised of mono-energetic gamma rays that range from 300 to 2000 keV, with a 100 keV interval. Tally output has an energy bin of 20 keV. This data set creates Green's function. It indicates the probability that a gamma photon of energy Ej will generate an energy flux in the detector. This is after passing through the detector and seat shielding. Now, to estimate the energy deposited by the flux in the detector, we need to multiply the Green function generated at various energies (ε) [14]. Fig. 1 shows a diagram of scattered photons created by input photon interaction with a shield. To obtain the detector response matrix, Green's function is multiplied by the detector's inherent efficiency.

To calculate the detector's intrinsic efficiency, the F6 Tally is used in the MCNP code. Tally f6 gives the energy stored per unit mass of

the detector, so the inherent efficiency of the detector can be obtained using equation 2:

$$\xi(\varepsilon) = \frac{(f6)}{(\varepsilon)} \times m_d \quad (2)$$

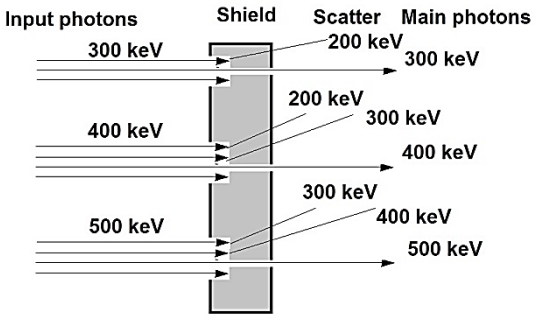

Fig. 1. Diagram of scattered photons created by the interaction of input photons with a shield.

where m_d is the mass of the sodium crystal (which is easily obtained in the MCNP output file after executing the code), ε is the source energy, f6 is the energy stored in the mass of the detector, and ξ (ε) is the inherent efficiency of the detector (the total energy stored in the crystal for a photon of a source with energy).

We used a 100 keV energy bin for folding. The mathematical description of this can be as follows:

$$S(\varepsilon_i) = \sum_j G(E_j \rightarrow \varepsilon_i) X(E_j) \xi(\varepsilon_i) \quad (3)$$

Where $G(E_j \rightarrow \varepsilon_i)$ Green's function which denotes the probability that a gamma photon of energy Ej will produce a flux of energy ε_i in the detector after passing through the shielding of detector and seat. $X(E_j)$ is the spectrum outside the shielding having the energy parameter as denoted by $\xi(\varepsilon_i)$ is the spectrum inside the shield with energies ε_i. The detector response matrix for a photon, which is obtained using the MCNP simulation, is obtained by the folding method described in Mitra et al. study [14].

Because of the presence of lead in shielding design, the simulation becomes a deep penetration problem, so variance reduction techniques are used to reduce the relative error [14]. We use Russian roulette and the splitting technique and find out the figure of merit (F) relative error (r_e), relative variance of variance (V_{OV}), and computer time (τ) for different splitting combinations at and ono energetic sources of 0.3, 0.5, 1.5 and 2.0 MeV. Table 1 gives a comparison of the values of the statistical indicators for different splitting combinations at 1.0 MeV source energy. These variances were considered for different tally types track length (t_F), energy deposition (t_E), and computation time (τ) in minutes for various combinations of cell importance.

Table 1. Values of statistical indicators for various combinations of cell importance: F, r_e and V_{OV} for different tally types track length (t_F), energy deposition (t_E), and computation time (τ) in minutes.

Combination	$F(t_F)$	$F(t_E)$	$r_e(t_F)$	$r_e(t_E)$	$V_{OV}(t_F)$	$V_{OV}(t_E)$	τ
1:1:1	60.21	59.85	0.0254	0.0255	0.001	0.0011	25.78
1:2:4	93.14	92.86	0.0241	0.0241	0.0014	0.00138	18.51
1:2:6	87.29	87.05	0.0251	0.0251	0.0017	0.0017	18.14
1:2:8	85.88	85.59	0.0255	0.0255	0.0018	0.0018	17.91
1:3:6	102.05	101.63	0.0226	0.0226	0.0014	0.0014	19.26
1:3:9	97.27	96.55	0.0231	0.0231	0.0017	0.0017	19.25
1:4:8	108.23	107.9	0.0213	0.0213	0.0013	0.0013	20.37

2.2 MCNPX modeling

The design of the whole-body counter with chair geometry includes a NaI (Tl) detector with 2 x 2 inches (5cm x 5cm), a lead collimator, and a BOMAB phantom. Fig. 2 shows the detector and collimator modeling, and Fig. Figure 3 illustrates the modeling of phantom and chair shielding by the MCNPX code. In this study, the MCNPX code was applied to evaluate particle transport between the source and the detector.

The reason for using a 2x2-inch NaI detector is to achieve a portable system with acceptable performance. This is because larger detectors require a larger collimator, which makes it heavier. The initial shield design is cylindrical, and the radiation inlet to the detector is conical. The shielding materials are iron, lead, copper, and cadmium (from the outside to the detector) with thicknesses of 3 mm, 5 cm, 2 mm, and 1 mm, respectively. Figure 1 shows shielding geometry modeling. Initially, for design purposes, a BOMAB phantom was used in the simulation. This consists of 10 bottles made of polyethylene or Plexiglas and contains a uniform distribution of radioactive liquid (cesium-137 or cobalt-60) [5]. In the MCNPX code, each energy was executed with 100 million particles in the program. Tally F8 was used to determine the number of counts in the all-energy peak region.

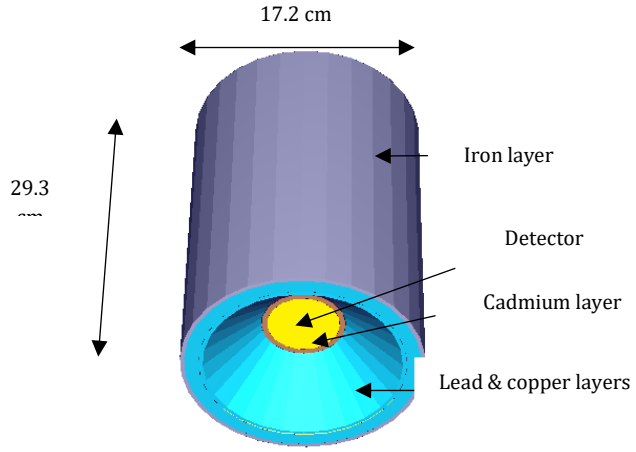

Fig. 2. The layout of the detector setup includes NaI (Tl) and shielding layers.

These steps were simulated for the θ= 45° relative to the horizon surface and a d= 70 cm from the detector to the phantom. According to the model based on the Monte Carlo method to estimate the background radiation spectrum presented in the reference, Mitra et al. study, the background radiation spectrum inside the shield for the geometry of the whole-body counter system is calculated using MCNP code [14]. To describe the background radiation, the simulated source is a spherical surface source that surrounds the entire whole-body counter system. Each point on this spherical surface acts as an isotropic point where the rays are emitted in the same direction in the sphere with the same probability. In Monte Carlo calculations, these points are randomly but uniformly distributed on the spherical surface. Although this model does not exactly resemble real background radiation, it can be simple and very close to background radiation. The choice of such a source avoids complexity. The spherical surface source is defined by the command *sur*; and the direction is considered inside the spherical surface. Figure 4 shows the simulated geometry of the counter system, which includes a surface source, shielded chair, detector, and collimator cell. Using f4 in the MCNPX code, the energy flux distribution inside the detector for the simulated geometry is calculated when the source (background radiation) is outside the shield and collimator. For this purpose, in the input file, single energy sources of gamma from the energy range of 300 keV to 2000 keV with an interval of 100 keV are considered, and the program is executed for each energy.

3. Results and discussion

In this section, to validate the input file for the MCNPX code, first a comparison was made between the results of efficiency calculations for two groups: this study and Kramer et al.'s study (Table 2). The detectors had dimensions D = 29.2 cm and H = 10.2, and a BOMAB phantom was used [16]. In comparison, Table 2 shows the maximum difference in efficiency is 9.1 % related to 364 keV photon energy. This difference can be due to density changes for different types of steel used in the detector window. The geometry of the detection in this simulation is such that the phantom is placed on a chair at an angle of 45° to the horizon and at a distance of 71 cm (Fig. 3).

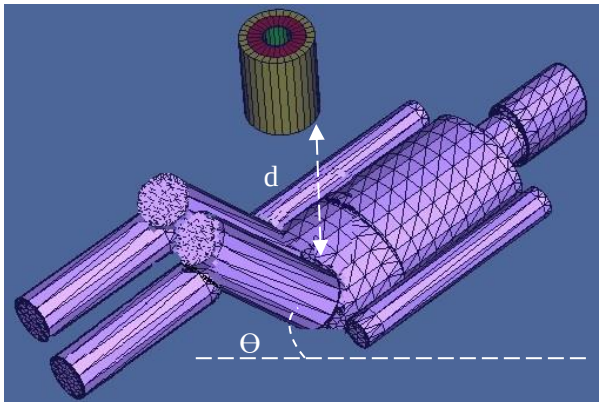

Fig. 3. Geometry of the detection setup used for MCNPX simulation includes a detector, shielding layers collimator and phantom with uniform distribution.

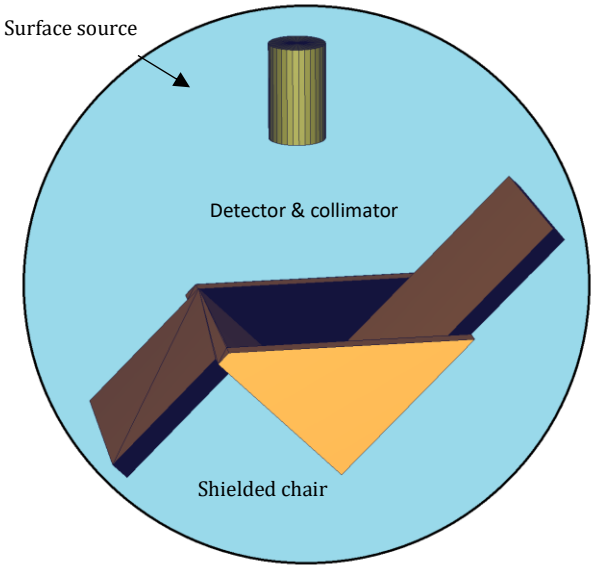

Fig. 4. Geometry of the counter setup used for MCNPX code. It includes surface source, shielded chair, detector and collimator.

The results of the simulation calculations for NaI (Tl) with a dimension of 2 x 2 inches in two cases, with and without a lead collimator, while located at a distance of 71 cm from the BOMAB phantom, are shown in Fig. 5. The detection geometry in this simulation is such that the phantom is placed on a chair at an angle of 45°. The efficiency of the detector decreases with increasing energy, and its values in the collimator are 10^{-4} to 10^{-5}. These results are consistent with published reports on commercial whole-body counters [5].

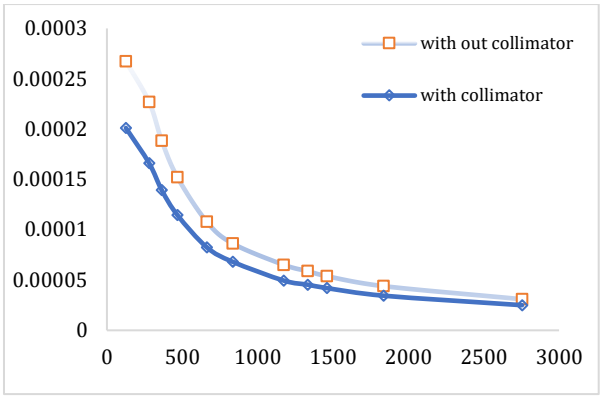

Fig. 5. The simulation calculations for NaI (Tl) with dimension of 2 x 2 inch in two cases, with lead collimator and without lead collimator.

The energy flux distribution inside the NaI (Tl) detector, represented as Green's function, $G(E_j \rightarrow \varepsilon_i)$, is shown in Fig. 6 for several different energies, which are calculated using the MCNPX code. These diagrams show that the most significant share of energy flux distribution inside the detector is due to the main beam of the source. Scattering beams also have a smaller share of energy flux inside the detector in the energy range than the main beam. The scattered beams are created by the interaction of the main beams with the shielding material.

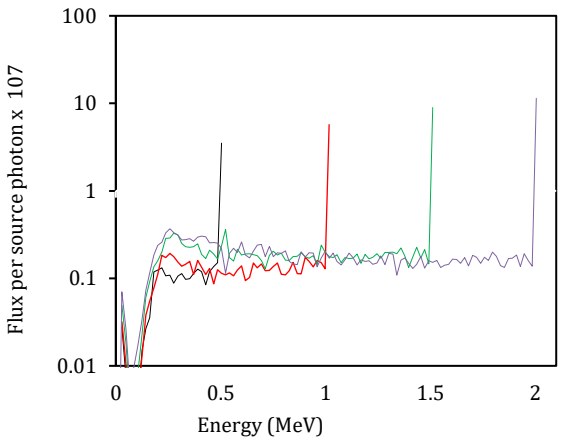

Fig. 6. Plot of the Green's function at source γ energies 0.5, 1.0, 1.5 and 2 MeV. This is the flux in the detector transmitted through the lead collimator for one source photon.

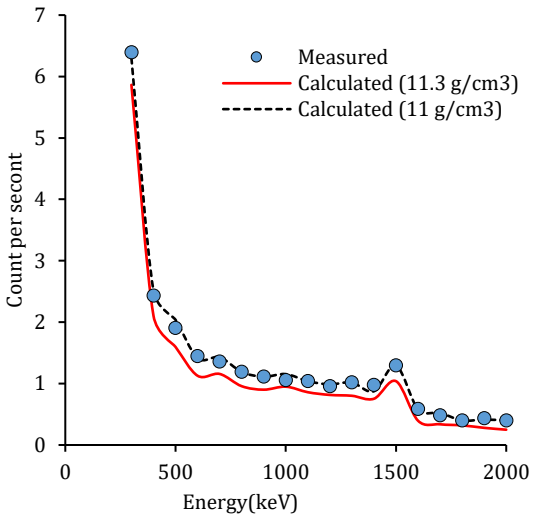

Fig. 7. Comparison of measured background γ-spectrum with simulated results for two different densities (11 and 11.3 gcm^{-3}) of lead.

Figure 7 illustrates the results of estimating the gamma spectrum of background radiation through simulation and experimental measurements. This is done by considering the lead collimator for the detector. The peaks observed in both spectra are from gamma rays resulting from the decay of potassium-40 in the environment. A comparison of the results with the results of the Mitra et al. study [13] indicates that the background radiation level in this study decreased in the order of 0.5 due to the use of a lead shield at an energy of 1400 keV. Fig. 8 shows the difference between the simulation and the measured results. We observe that the calculated spectrum underpredicts the measured spectrum at all energies even though corrections for detector efficiency have been made, and the difference between the two spectra is prominent at higher energies due to the porosity of the lead shielding. One of the reasons for this difference may be due to the fact that in simulations, a spherical surface source is considered a background radiation source. Another reason may be that, in the simulation, lead density was considered highly uniform and pure. In the real world, there may be a series of pores and impurities in the lead that reduce its effective density. Figure 8 shows the flux changes for different lead densities and single-energy sources. Therefore, the detector response matrix (Fig. 3) is obtained for lower densities, which results in the fact that the effective density of 11 g.cm^{-3} gives the best match between the measured and simulated background radiation (Fig. 8). The maximum relative error for simulation data in Figure 8 is 1.99%, which corresponds to the 300keV gamma energy.

Because of the presence of the lead shield in this study, there is a problem with deep penetration. This results in a large statistical error. Then, the use of variance reduction techniques in Monte Carlo simulations is highly recommended for such cases.

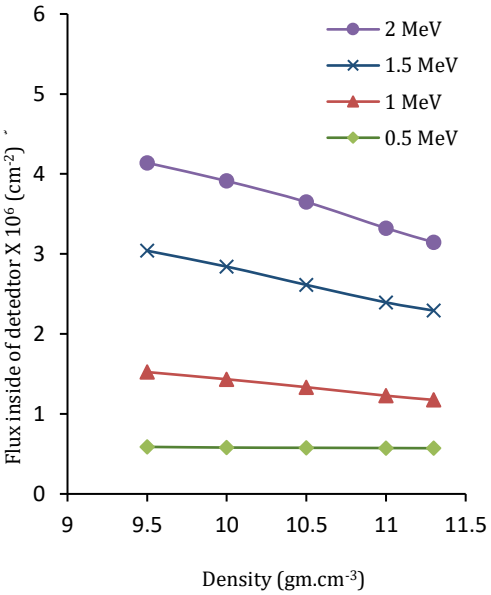

Fig. 8. Flux changes in the detector after passing through the shield with different densities and energies.

Table 3 compares, the MDA values calculated in this study were compared with Kramer et al.'s study [23]. Due to the larger detector dimensions (7.5 cm x 7.5 cm) in Kramer et al. study, the counting efficiency values are about 7 to 12 times larger than the efficiency values in this study (detector size of 5 cm x 5cm). However, the background counts in this study are lower due to the proper lead shielding. As

shown in Table 3, we will eventually have an estimate of the MDA values for the desired energy. Although the small detector is usually used for thyroid monitoring, we have shown that it can also be used in the whole-body counter in emergencies. In this method, without the need for costly experimental tests, we can only use Monte Carlo calculations to determine the shield's contribution to improving the MDA value. The design of such a counter system allows screening a large-scale radiological incident with MDA values of about 1-4 kBq. However, the results of the measurement can be used for rapid estimation of internal contamination.

In order to simulate the source for background radiation, a spherical surface source was surrounding the setup. This is an approximate way to describe the actual background. Also, features such as nonlinearity of scintillation efficiency and single escape peak shift need to be taken into account to achieve an accurate result.

Sahrma et al. have used simulation tools to understand the shielding effectiveness. [24]. In the case of outdoor open fields, natural background radiations were simulated with the assumption of an infinite half-space source, which means a 2π- source geometry, and for intense γ-rays emitted by long-lived radioactive nuclei, like ^{40}K, ^{232}Th, and ^{226}Ra or their progenies. They mentioned that indoor source geometry is difficult to realistically model. It seems that the method used in this study can be applied to the topics that are discussed in practice above.

Table 3. Comparison of the MDA values (Bq) in a NaI (Tl) counter between this study and Kramer et al study [23] that counting time was 5min.

E (keV)	Efficiency (count /photon)		Background (cps)		MDA	
	This study	Kramer study	This study	Kramer study	This study	Kramer study
280	1.66×10^{-4}	1.17×10^{-3}	7.15	24.50	4320	1137
364	1.39×10^{-4}	1.06×10^{-3}	3.85	17.03	3780	1044
468	1.14×10^{-4}	9.33×10^{-4}	2.26	10.47	3540	931
662	8.26×10^{-5}	7.68×10^{-4}	1.41	10.17	3860	1114
834	6.81×10^{-5}	6.77×10^{-4}	1.16	8.22	4240	1137
1173	4.94×10^{-5}	5.59×10^{-4}	0.98	6.83	5380	1255
1332	4.54×10^{-5}	5.20×10^{-4}	1.00	7.13	5910	1380
1460	4.19×10^{-5}	4.91×10^{-4}	1.01	7.78	6440	1527
1836	3.44×10^{-5}	4.21×10^{-4}	0.41	1.87	4990	871

4. Conclusions

Evaluation of detector efficiency and background radiation was performed to design a whole-body counting system with chair geometry equipped with a NaI (Tl) detector using the MCNPX code. In the case of outdoor open fields, natural background radiations were simulated and the source input was considered mono-energetic gamma rays that range from 300 to 2000 keV. This type of detailed simulation becomes a useful tool for simulating

background in low-level counting setups. Any modification in the background spectrum can be incorporated by simply multiplying the Green's function with the probability distribution of the measured spectrum. Computational data were used to estimate the monitoring system MDA. This method is cheaper to design and test a counter system for low-level counting of γ emitting radionuclides than experimental methods.

References

1. Mizushita S. Portable Chair Type Whole-Body Counter. J. Nucl Sci Technol. 1977;14:911-915.
2. Shagina NB, Bougrov NG, Degteva MO, Kozheurov VP, Tolstykh EI. An Application of Invivo Whole Body Counting Technique for Studying Strontium Metabolism and Internal Dose Reconstruction for the Techa River Population. Phys Conf Ser. 2006;41:433–440.
3. Mizushita S. New Chair type Whole-body Counter. J. Nucl Sci Technol. 1989;26:278-285.
4. Ishikawa T, Matsumoto M, Uchiyama M. A Calibration Method for Whole-body ounters, Using Monte Carlo simulation. Radiat Prot Res. 1996;64:283-288.
5. Bento J, Barros S, Teles P, Neves M, Gonçalves I, Corisco J, Vaz P. Monte Carlo Simulation of the Movement and Detectable Efficiency of a Whole Body Counting System Using a BOMAB Phantom. Radiat Prot Res. 2012;148:403–413.
6. Shi H, Chen B, Li T, Yun D. Precise Monte Carlo Simulation of Gamma-ray Response Functions for a NaI (Tl) Detector. Appl Radiat Isot. 2002;5:517-524.
7. Kim J, Lee B, Choi H, Lim Y. Efficiency Calibration of Bed Type Whole-body Counter Using Monte Carlo Simulations and Application to Intake Estimation of 131I. J. Nucl Sci Technol, 2011;1:549-551.
8. Gouda MM, Badawi MS, El-Khatib AM, Hussien N. Calculation of NaI (TI) Detector Full-Energy Peak Efficiency using the efficiency transfer method for Small radioactive cylindrical Source. Nucl Technol Radiat Prot. 2013; 31:150-158.
9. Schlagbauer M, Hrnecek E, Rollet S, Fischer H, Brandl A, Kindlet P. Uncertainty Budget for a Whole-body Counter in the Scan Geometry and Computer Simulation of the Calibration Phantoms. Radiat Prot Dos. 2007;125:149-52.
10. Ören Ü, Andersson M, Rääf C, Mattsson S. A phantom for determination of calibration coefficients and minimum detectable activities using a dual-head gamma camera for internal contamination monitoring following radiation emergency situations. Radiat. Prot. Dosim. 2016; 169: 297–302.
11. Díaz-Londoño G, García M, Astudillo R, Hermosilla A. Development and implementation of tools for self-monitoring of staff exposed to 131I in nuclear medicine centres of Chile. Radiat. Prot. Dosim. 2017. 173 (4), 302–307.
12. Medici S, Desorgher L, Carbonez P, Damet J, Bochud F, Pitzschke A, Impact of the phantom geometry on the evaluation of the minimum detectable activity following a radionuclide intake: From physical to numerical phantoms. Radiat Measur. 2020;139: 106485.
13. Santos R, Xavier M, Cardoso JCS. Evaluation of The Minimum Detectable Activity of Whole Body and Thyroid Counters at In Vivo Monitoring Laboratory of IPEN/CNEN-SP. International Nuclear Atlantic Conference – INAC, 2011.
14. Mitra MS, Sarkar PK, Monte Carlo Simulations to Estimate the Background Spectrum in a Shielded NaI (Tl) γ-Spectrometric System. Appl Radiat Isot. 2005;63:415-422.
15. Estrada JJ, Laurer GR A Method to Obtain Subject Background for Low level In-vivo Measurements of the Head. Health Physics Society. 1993; 306-312.
16. Kramer G, Crowley P, Burns LC. Investigating the Impossible: Monte Carlo Simulations. Radiat Prot Dos. 2000; 89:259-262.
17. Breustedt B, Eschner W. Monte Carlo Calibration of Whole-body Counters with NaI (Tl) Detectors in Stretcher Geometry. Radiat Prot Dos. 2010;139: 510-518.
18. Tariq H, Mirza S, Rehman S, Mirza NM. Stochastic Simulation Study of HPGe Detector Response and the Effect of Detector Aging Using Geant4, Nucl Technol Radiat Prot. 2017;32, 57-69.
19. Kinase S, Yoshizawa M, Kuwabara J, Noguchi H. Evaluation of Response of Whole-body counters using the EGS4 Code. Nucl Sci Technol. 1998; 35:958-962.
20. Kramer G, Capello K, Ross K, The W-chair Whole Body Counter: a Monte Carlo Investigation. Health Phys. 2005; 88:364-370.

21. Lei W, Yi-ni W, Jie P, Jing N, Xin L, Xue-lan Y, Ting Z, Wei L, Xian-guo T. A portable internal contamination monitor with dual detectors for screening in a large-scale radiological incident. Appl Radiat Isot. 2019; 154:108858.
22. Poorbaygi H, S Pourali, Mostajabodavati M, Bagheri S , Design and Calibration of a Chair-Type Whole Body Counter. Iranian J. Nucl Sci Technol. 2016;78:18-23.
23. Kramer, G, and Capello, K. Calibration of the HML's portable whole body counter as a function of BOMAB phantom size and energy modelled by MCNP. Spain: N. p., 2004. Web.
24. Sharma S, Sarkar MS. Measurement and simulation of gamma-ray background in a low energy accelerator facility, J. Instrumen. 2020;:15;1-19.

How to cite this article

H. Poorbaygi, S. Pourali, K. Moradi, *Evalution of Minimum Detection Activity in a Portable whole Body Counter Using Monte Carlo Method*, Journal of Nuclear Science and Applications (JONRA) Volume 4 Number 1 Winter (2024) 45-53.
URL: https://jonra.nstri.ir/article_1626.html**, DOI**: https://doi.org/10.24200/jon.2024.1004.